



Targeting the vasopressin type-2 receptor for renal cell carcinoma therapy

Sonali Sinha^{1,2} · Nidhi Dwivedi^{1,2} · Shixin Tao^{1,2} · Abeda Jamadar^{1,2} · Vijayakumar R. Kakade^{1,2} · Maura O' Neil³ · Robert H. Weiss^{4,5} · Jonathan Enders⁶ · James P. Calvet^{1,7,8} · Sufi M. Thomas^{8,9} · Reena Rao^{1,2,8}

Received: 7 September 2018 / Revised: 30 September 2019 / Accepted: 3 October 2019 / Published online: 15 October 2019
© The Author(s), under exclusive licence to Springer Nature Limited 2019

Abstract

Arginine vasopressin (AVP) and its type-2 receptor (V2R) play an essential role in the regulation of salt and water homeostasis by the kidneys. V2R activation also stimulates proliferation of renal cell carcinoma (RCC) cell lines in vitro. The current studies investigated V2R expression and activity in human RCC tumors, and its role in RCC tumor growth. Examination of the cancer genome atlas (TCGA) database, and analysis of human RCC tumor tissue microarrays, cDNA arrays and tumor biopsy samples demonstrated V2R expression and activity in clear cell RCC (ccRCC). In vitro, V2R antagonists OPC31260 and Tolvaptan, or V2R gene silencing reduced wound closure and cell viability of 786-O and Caki-1 human ccRCC cell lines. Similarly in mouse xenograft models, Tolvaptan and OPC31260 decreased RCC tumor growth by reducing cell proliferation and angiogenesis, while increasing apoptosis. In contrast, the V2R agonist dDAVP significantly increased tumor growth. High intracellular cAMP levels and ERK1/2 activation were observed in human ccRCC tumors. In mouse tumors and Caki-1 cells, V2R agonists reduced cAMP and ERK1/2 activation, while dDAVP treatment had the reverse effect. V2R gene silencing in Caki-1 cells also reduced cAMP and ERK1/2 activation. These results provide novel evidence for a pathogenic role of V2R signaling in ccRCC, and suggest that inhibitors of the AVP-V2R pathway, including the FDA-approved drug Tolvaptan, could be utilized as novel ccRCC therapeutics.

Introduction

Renal cell carcinoma (RCC) is the most common cancer of the kidneys, arising from tubular epithelial cells within the renal cortex. It is the eighth leading cause of cancer related fatalities with 15,000 deaths and 65,000 new cases detected

per year in the United States [1]. Despite surgical, immunotherapy, and chemotherapy interventions, the 5-year survival rate is only 8% for stage 4 RCC patients. RCCs occur in multiple histologically and genetically heterogeneous subtypes of which, clear cell RCC (ccRCC) represents 80% of the cases of RCC [2]. ccRCC tumor cells are highly invasive, metastatic, and resistant to radiation and chemotherapy [2]. Hence, a better understanding of the mechanisms that drive ccRCC pathogenesis could help in the development of new, and more effective therapies for ccRCC.

Supplementary information The online version of this article (<https://doi.org/10.1038/s41388-019-1059-0>) contains supplementary material, which is available to authorized users.

✉ Reena Rao
rrao@kumc.edu

¹ The Jared Grantham Kidney Institute, University of Kansas Medical Center, Kansas City, KS, USA

² Department of Internal Medicine, University of Kansas Medical Center, Kansas City, KS, USA

³ Department of Pathology and Laboratory Medicine, University of Kansas Medical Center, Kansas City, KS, USA

⁴ Division of Nephrology and Comprehensive Cancer Center, University of California, Davis, CA, USA

⁵ Medical Service, VA Northern California Health Care System, Sacramento, CA, USA

⁶ Department of Anatomy and Cell Biology, University of Kansas Medical Center, Kansas City, KS, USA

⁷ Department of Biochemistry and Molecular Biology, University of Kansas Medical Center, Kansas City, KS, USA

⁸ Department of Cancer Biology, University of Kansas Medical Center, Kansas City, KS, USA

⁹ Department of Otolaryngology, University of Kansas Medical Center, Kansas City, KS, USA

Arginine vasopressin (AVP) or antidiuretic hormone is produced mainly by the hypothalamus and released into the blood from the pituitary. To elicit its actions in target organs, it binds to its type-1 (V1aR and V1bR) and type-2 (V2R) G-protein-coupled receptors (GPCRs). V2R is normally expressed in the renal collecting duct, distal tubule, and thick ascending limb segments of renal nephrons, where it plays an essential physiological role in regulating water and electrolyte homeostasis [3]. However, ectopic expression of AVP and its receptors has been reported in breast, pancreatic, colorectal and gastrointestinal cancers, and small-cell lung carcinoma [4, 5]. While V1R activation has been observed to increase tumor cell growth [6, 7], V2R agonists are generally known to have angiostatic, anti-proliferative and/or antimetastatic effects in breast, lung, and colorectal cancers [8–10]. However, in contrast to these protective roles of V2R, one study reported that V2R activation increased cell proliferation of ccRCC cell lines of human origin *in vitro* [11]. This finding is notable because ccRCC is thought to originate from proximal tubules [12–15], which normally does not express V2R [16].

While it appears that V2R activation may be proproliferative in cultured RCC cell lines, it is not known if V2R is expressed and active in human RCC tumors *in vivo*. It is also not known which RCC subtypes express V2R; if AVP-V2R cell signaling regulates RCC tumor growth; or if V2R is potentially a viable target for therapeutic inhibition in RCC. As such, in the current study, we asked whether AVP-V2R signaling is pathogenic in RCC, and tested the therapeutic potential of targeting V2R for inhibition in this malignancy both *in vitro* and *in vivo*.

Results

Abnormal V2R expression in human tumors

To determine the possible clinical relevance of V2R expression in cancer, we first examined the pan-cancer gene expression of V2R (AVPR2 gene) and its ligand, AVP, in the TCGA database. AVPR2 was found to be upregulated in cancers of the breast, bladder, colon, lung, ovary, pancreas, prostate, skin, thyroid, thymus, head, and neck, and in sarcoma and diffuse large B-cell lymphoma, with kidney cancer being one of the major expressors (Fig. 1a). Among the limited number of cancer types covered by the index, higher AVP gene expression was restricted to cancers of the kidney, adrenocortical, bladder, and liver (Fig. 1b). AVPR2 and AVP gene expression were detected in chromophobe, papillary, and ccRCC (Supplementary Fig. 1a, b). Hence, to further examine the role of V2R in RCC, we next determined its expression in human RCC cell lines and tumors.

V2R mRNA expression was detected in 14 out of 27 human ccRCC tumors using a commercially available cDNA array, (Fig. 1c), whereas only 1 out of 12 human papillary RCC tumors showed V2R expression (Supplementary Fig. 2a). V2R expression was also observed in nearly all cDNA samples that we isolated from primary human ccRCC tumor biopsy samples (Supplementary Fig. 2b). Although kidneys are not normally known to secrete AVP, many tumors are known to acquire the capacity to secrete neuropeptides [17]. Hence, to determine if in addition to ectopic V2R expression, ccRCC tumors can also produce its ligand, we examined AVP mRNA levels. AVP expression was detected in 12 out of 27 human ccRCC tumors in the cDNA array (Fig. 1c) and 2 out of 8 human ccRCC tumor biopsy samples (Supplementary Fig. 2c). AVP was also detected in 5 out of 12 human papillary RCC tumors in the cDNA array (Supplementary Fig. 2a). V1R mRNA was detected in all human ccRCC and papillary tumors (Supplementary Fig. 2a, b, e).

Immunostaining to detect V2R protein expression in ccRCC tumor tissue sections showed cell membrane associated V2R in tumor cells, but not in the tumor stroma (Fig. 1d). In the nonmalignant control kidneys, cells of the proximal tubules did not express V2R (Fig. 1d). In a tumor tissue microarray of RCC tumor sample cores from different patients, 156 out of 162 ccRCC samples showed V2R expression (Fig. 1e). V2R expression in ccRCC tumor cores also increased with increasing clinical tumor grade (Fig. 1f) and TNM values (Fig. 1g). V2R mRNA was also detected in Caki-1, 786-0, and ACHN human RCC cell lines (Fig. 1h). V1R was found to be expressed in control HK-2 cells lines, compared with which, Caki-1, 7860, and ACHN cell lines showed relatively lower V1R expression (Supplementary Fig. 2d).

V2R is normally expressed in kidney collecting ducts, distal tubules, and thick ascending limbs, but not in proximal tubules [16]. As expected, we detected V2R mRNA in nonmalignant control kidney tissue using cDNA array (Fig. 1c, Supplementary Fig. 2b) and by immunostaining of tissue sections (Fig. 1d, e). V2R was not detected in the HK-2 human proximal tubule cell line (Fig. 1h), or in the proximal tubules of nonmalignant control kidney tissues (Fig. 1d). These results demonstrate that the expression of V2R and its ligand, AVP in human ccRCC tumors is ectopic and abnormal.

V2R antagonists inhibit growth of ccRCC cell lines *in vitro*

To determine the possible role of V2R in tumor cell survival, proliferation, and migration, *in vitro* studies were carried out. Treatment with the V2R antagonist OPC31260 for 48 h dose-dependently reduced cell viability of 786-O

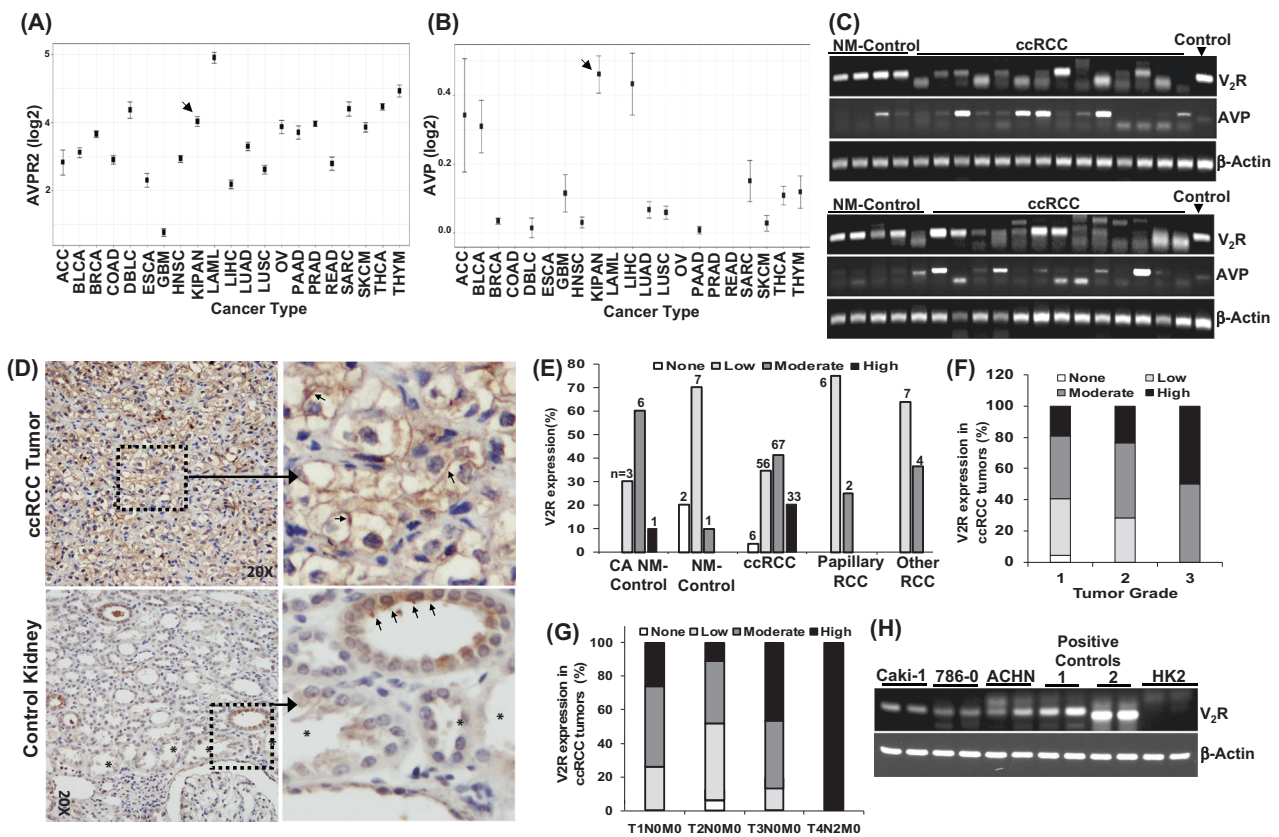


Fig. 1 V2R expression and cell signaling in human RCC tumors: **a** Pan-cancer V2R (AVPR2 gene) and **b** AVP gene expression determined from the TCGA database. Black arrow depicts levels in Pan-kidney cancer (KIPAN). Other tumor types assessed include adrenocortical carcinoma (ACC), bladder (BLCA), breast (BRCA), colon (COAD), diffuse large B-cell lymphoma (DLBC), esophageal carcinoma (ESCA), head and neck (HNSC), acute myeloid leukemia (LAML), liver hepatocellular carcinoma (LIHC), lung adenocarcinoma (LUAD), lung squamous cell carcinoma (LUSC), ovarian (OV), pancreatic adenocarcinoma (PAAD), prostate adenocarcinoma (PRAD), rectum adenocarcinoma (READ), sarcoma (SARC), skin cutaneous melanoma (SKCM), thyroid carcinoma (THCA), and thymoma (THYM). **c** RT-PCR for V2R, AVP, and β -actin using a cDNA array of human nonmalignant control (NM-control) kidney and ccRCC

tumors. Caki-1 cell and mouse pituitary lysate are used as positive controls respectively for V2R and AVP respectively. **d** Immunostaining for V2R in human ccRCC tumor or NM-control kidney samples. Asterisk represents proximal tubules and arrows point to cells showing V2R staining (brown). **e** Pathologist's scoring of V2R expression in tissue microarray. Numbers in the graph represent the number of tissue core samples. **f** The percentage of ccRCC tumors with V2R expression in different tumor grades and **g** different TNM staging. **h** RT-PCR for V2R and β -actin in cultured Caki-1, 786-O, and ACHN human RCC cell lines. Positive controls 1 and 2 represent cystic epithelial cells from human polycystic kidney disease kidneys and 18 h water-deprived mouse kidneys, respectively. The HK-2 human proximal tubule cell line is a negative control

and Caki-1 cells as determined by the MTT assay, with a 50% reduction noted at 5–10 μ M doses (Fig. 2a). No significant change in cell viability was noted at 24 h under similar treatment conditions. In contrast to ccRCC cells, control HK-2 cells had significantly higher survival (over 92%) at the same doses of OPC31260 (Supplementary Fig. 3a). A significant decline in colony formation was also observed starting at 5 and 10 μ M doses of OPC31260 for 786-O and Caki-1 cells, respectively (Fig. 2b, c). Cell cycle analysis revealed that 60–70% of 786-O and Caki-1 cells treated with 10 μ M or higher doses of OPC31260 were in the G2/M cell cycle phase, suggesting G2/M cell cycle arrest (Fig. 2d, e, f). However, OPC31260 treatment caused only a small increase in apoptosis in these cells (Supplementary Fig. 3b, c). OPC31260 treatment also dose-

dependently reduced wound repair of 786-O and Caki-1 cell monolayers (Fig. 2g, h). These results suggest that inhibition of V2R in ccRCC cells reduces clonogenicity and is cytostatic, and that inhibition of cell proliferation occurs by inducing G2/M cell cycle arrest rather than lytic death.

To further confirm the role of V2R in ccRCC cell growth, we also tested the effect of another V2R antagonist, Tolvaptan. Tolvaptan is a Food and Drug Administration (FDA) approved drug used to treat hyponatremia [18], and was recently approved to treat polycystic kidney disease (PKD) [19]. Caki-1 cells treated with increasing doses of Tolvaptan showed a significant reduction in cell viability (Fig. 2i) and wound closure (Fig. 2j, Supplementary Fig. 3d) starting at a dose of 10 μ M. Treatment of Caki-1 cells with dDAVP, a V2R agonist showed a trend towards

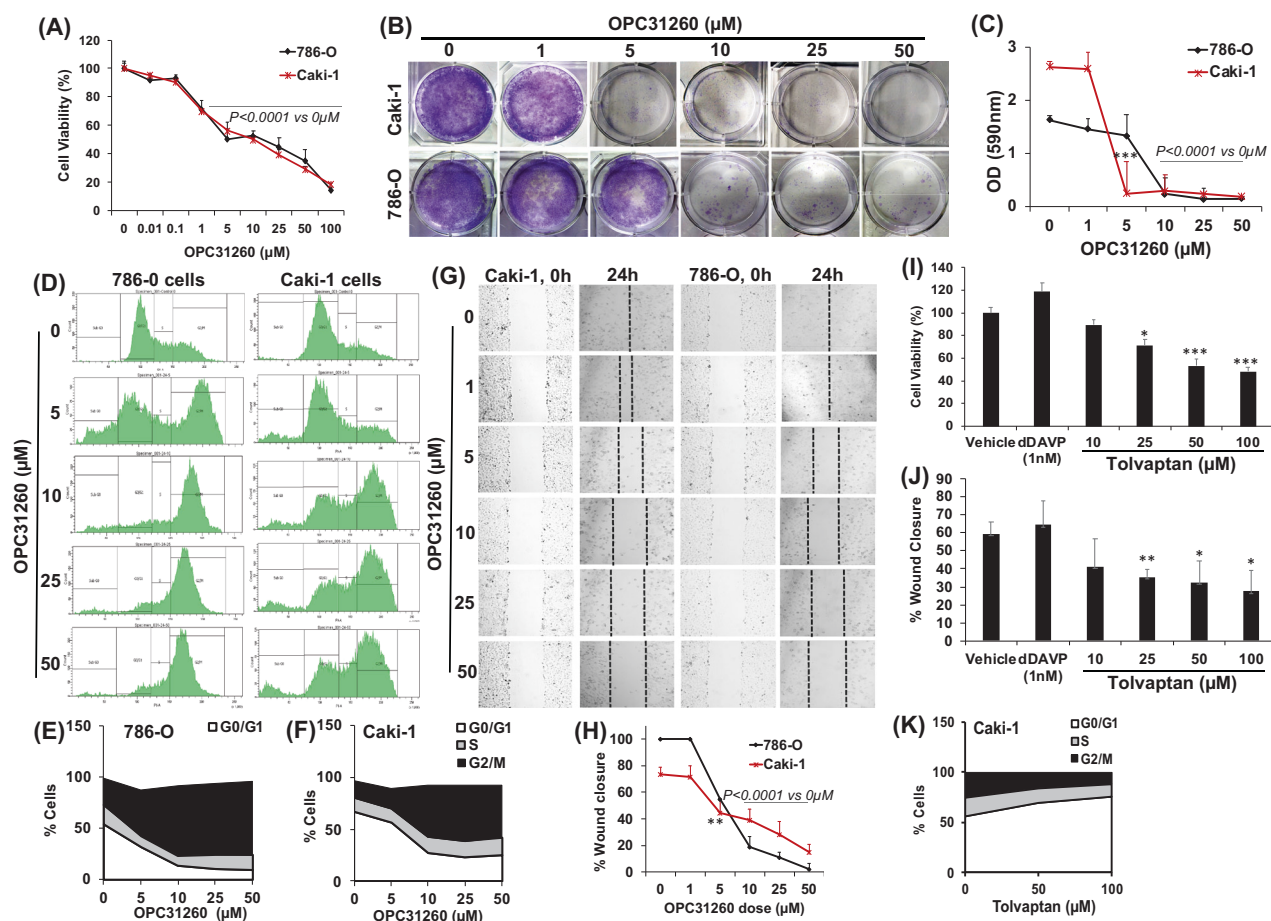


Fig. 2 Effect of V2R antagonists on growth of RCC cell lines: **a** Cell viability of 786-O, and Caki-1 cells treated with OPC31260 for 48 h measured by the MTT assay. **b** Representative images of clonogenic assays, of Caki-1 and 786-O cell lines treated with OPC31260. **c** Quantification of OPC31260-resistant colony formation. $***P < 0.001$ vs $0 \mu\text{M}$ OPC31260. **d** Representative histograms and **e** quantification of cell cycle stages in 786-O and **f** Caki-1 cells treated with OPC31260 (24 h), measured by FACS analysis of propidium iodide stained cells. **g** Representative images of the wound healing assay at 0 and 24 h after the scratch was placed on monolayers of Caki-1 and 786-O cells in the presence of different doses of OPC31260, and **h** quantitation of their

percent wound closure. $**P < 0.01$ vs $0 \mu\text{M}$ OPC31260. **i** Cell viability of Caki-1 cells treated with dDAVP or Tolvaptan for 48 h measured by the MTT assay. **j** Percent wound closure of Caki-1 cells, 24 h after the scratch was placed in the presence of dDAVP or Tolvaptan. **k** Quantification of cell cycle stages in Caki-1 cells treated with Tolvaptan. All error bars represent SD. $*P < 0.05$ $**P < 0.01$, and $***P < 0.001$ vs vehicle or $0 \mu\text{M}$ V2R antagonist. P values by one-way ANOVA followed by Dunnett's multiple comparison test for **a**, **c**, **h**, and two-tailed unpaired Student's t test with Welch's correction and F test in **i**, **j**

increased cell viability and wound closure when compared with vehicle treatment, but the values were not significantly different (Fig. 2i, j). Unlike OPC31260, Tolvaptan did not induce G2/M cell cycle arrest. Instead, Tolvaptan treatment at 50 and 100 μM for 24 h showed 18 and 26% increases in the numbers of cells in G0/G1 (Fig. 2k).

The V2R antagonist OPC31260 suppressed ccRCC tumor growth in a mouse xenograft model

To determine if V2R is a therapeutic target for ccRCC, the effect of OPC31260 was examined. For the studies, Caki-1 cells, which express V2R (Fig. 1c), were implanted subcutaneously in nude mice. Within 10 days, small tumors

expressing V2R (Supplementary Fig. 4a) appeared. Mice carrying tumors of ~ 80 – 100 mm^3 size were randomized into three groups for treatment with vehicle, OPC31260 (30 mg/Kg) or OPC31260 (60 mg/Kg) for 28 days by daily intraperitoneal injections. Tumor volumes in the vehicle treatment group increased steadily, and by day 28 were 7.8-fold higher than on day 1 (Fig. 3a). In contrast, the tumor volumes in the OPC31260 treatment groups failed to even double in size after 28 days of treatment (Fig. 3a). At sacrifice, the tumors in the OPC31260 treatment groups were smaller and weighed significantly less than in the vehicle treatment group (Fig. 3b, c). No significant difference in tumor volumes or weights were observed between the mice treated with 60 mg/Kg or 30 mg/Kg doses of

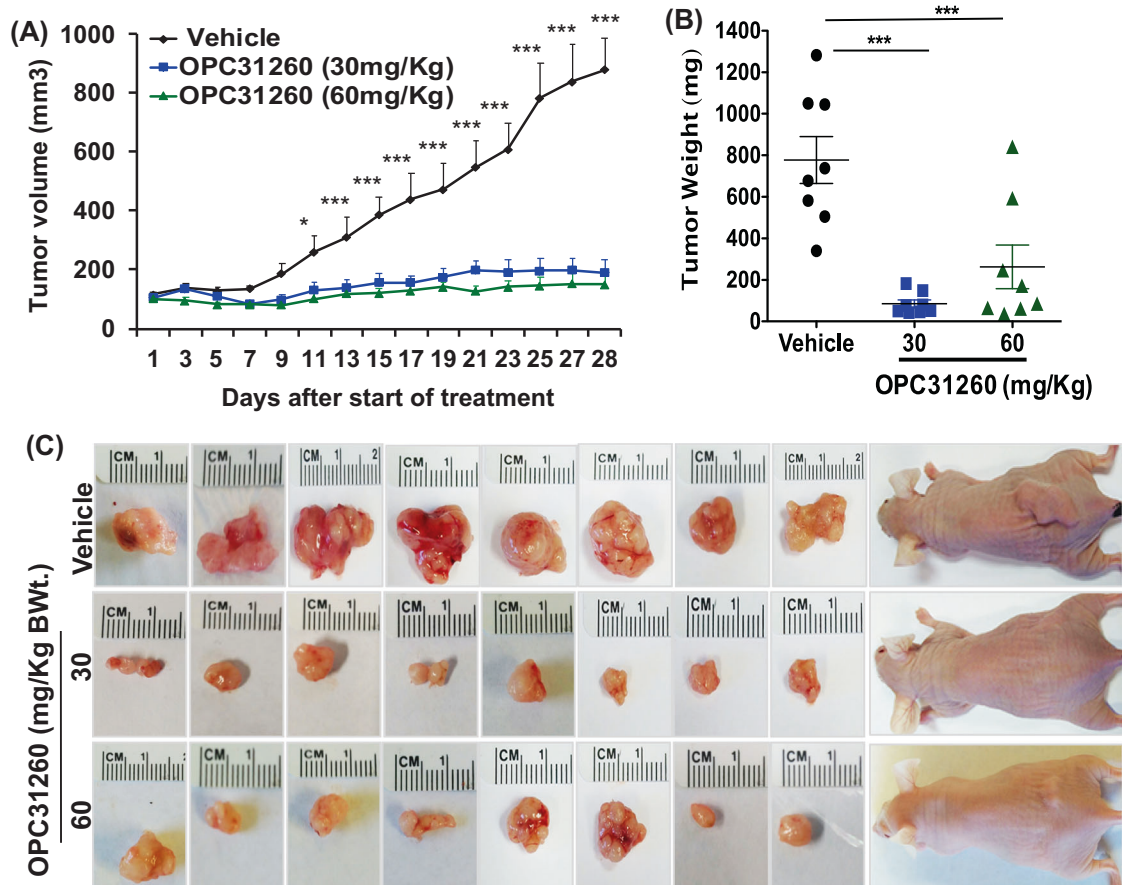


Fig. 3 The effect of OPC31260 on RCC tumor progression: **a** Nu/Nu mice were inoculated subcutaneously with Caki-1 cells, and 10 days later were treated with vehicle or OPC31260 (30 or 60 mg/Kg) for 28 days. Tumor volume is shown. **b** Images of tumors and mice with tumors at sacrifice. **c** Tumor weights at sacrifice. * $P < 0.05$, *** $P < 0.001$

vs OPC31260 (30 or 60 mg/Kg) in **a** and vs vehicle in **c**, ($n = 8$ mice/group). All error bars represent SEM. P values by two-way repeated measures of ANOVA followed by the Bonferroni test for **a**, and one-way ANOVA followed by Dunnett's multiple comparison test for **b**

OPC31260 (Fig. 3a, b). These results suggest that V2R could play a pathogenic role in ccRCC, and that its inhibition can reduce tumor growth in mice. OPC31260 treatment did not significantly affect the body weight of the mice, but reduced urine osmolality, as expected, in a dose-dependent manner (Supplementary Fig. 4b, c), suggesting that OPC31260 at these doses is well tolerated, but inhibits the V2R-regulated urine concentrating ability in these mice.

Tolvaptan suppressed ccRCC tumor growth, while dDAVP promoted tumor growth in a mouse xenograft model

To determine if Tolvaptan can be repurposed for RCC therapy, we tested its effect on tumor development in mice. In addition, the effect of dDAVP, a V2R selective agonist on tumor development was also tested. As before, Caki-1 cells were implanted subcutaneously in nude mice, and following tumor growth, mice were randomized into three groups: vehicle, Tolvaptan (120 mg/Kg by

daily oral gavage), or dDAVP (1 μ g/Kg by daily IP injection) for 28 days. As in the previous study, the tumor volumes in the vehicle treatment group increased by eightfold when compared with day 1 (Fig. 4a), while in the Tolvaptan treatment group, tumor volumes increased only by twofold (Fig. 4a). By comparison, tumor volumes in dDAVP treatment group significantly increased starting on day 21, and by day 28 were 14-fold higher than on day 1 (Fig. 4a). At sacrifice, the tumors in the Tolvaptan group were smaller and weighed significantly less when compared with the vehicle group, while the tumors were significantly larger in the dDAVP group (Fig. 4b, c). Tolvaptan and dDAVP treatment did not significantly change the body weight of the mice, but as with OPC31260 treatment, urine osmolality was significantly reduced by Tolvaptan treatment and increased by dDAVP treatment (Supplementary Fig. 5a, b), indicating that these AVP analogs were having their expected effects on urine concentrating ability with minimal obvious toxicity.

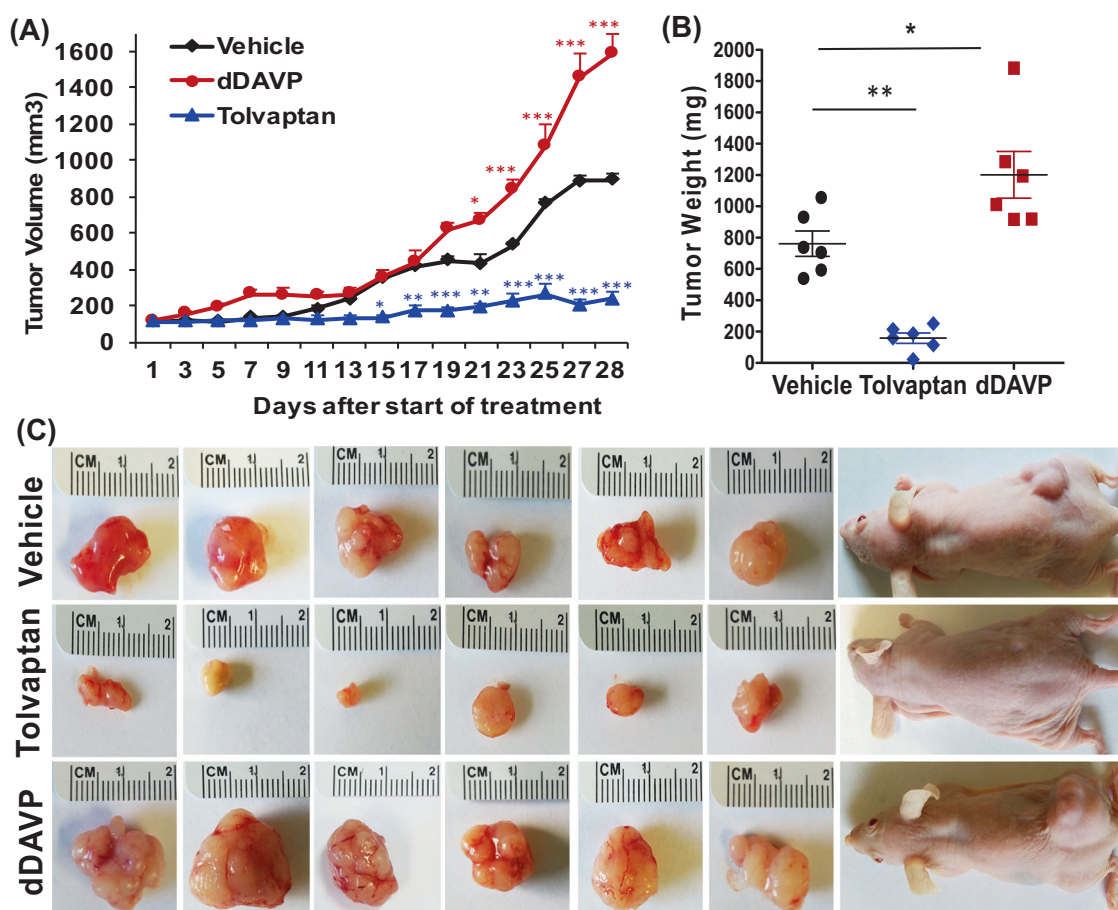


Fig. 4 Effect of Tolvaptan or dDAVP treatment on RCC tumor progression: **a** Nu/Nu mice were inoculated subcutaneously with Caki-1 cells, and 10 days later were treated with vehicle, Tolvaptan (120 mg/Kg), or dDAVP (1 μ g/Kg) daily for 28 days. **a** Tumor volumes, **b** tumor weights, and **c** representative images of tumors and mice with

tumors at sacrifice ($n = 6$ mice/group). $*P < 0.05$, $**P < 0.01$ vs vehicle ($n = 6$ mice/group). All error bars represent SEM. P values by two-way repeated measures of ANOVA followed by the Bonferroni test for **a** and one-way ANOVA followed by Dunnett's multiple comparison test for **b**

V2R antagonists reduced tumor cell proliferation and VEGF levels, and increased apoptosis in vivo

To determine the effect of Tolvaptan and OPC31260 on tumor cell growth, we measured cell proliferation and apoptosis in the tumors obtained from the above in vivo studies. In both the OPC31260 and Tolvaptan groups, the tumors showed significantly reduced Ki-67 staining (Fig. 5a, b), and increased TUNEL staining (Fig. 5a, c) compared with vehicle treatment. In contrast, tumors in the dDAVP group showed a significant increase in Ki-67 staining and reduced TUNEL staining compared with the vehicle group (Fig. 5a, b, c). Tumor microvessel density, determined by staining for CD31, was significantly reduced by OPC31260 treatment and increased by dDAVP treatment (Fig. 5a, d). Tolvaptan treatment did not appear to alter tumor microvessel density. However, OPC31260 and Tolvaptan significantly reduced VEGF protein levels, an important angiogenic growth factor in the tumors compared with

vehicle treatment (Fig. 5e, f), while dDAVP did not affect VEGF levels. These results suggest that V2R inhibition can reduce angiogenesis and tumor cell proliferation, and increase apoptosis in ccRCC tumors. To further test the effect of V2R inhibition on VEGF expression in ccRCC cells, we treated Caki-1 cells with OPC31260 and Tolvaptan. VEGF protein levels were unaffected in Caki-1 cells treated for 16 h with dDAVP, but were significantly reduced by Tolvaptan and OPC31260 (Fig. 5g).

V2R activity stimulates mitogenic cell signaling and cell growth in ccRCC

To examine V2R postreceptor mechanisms in ccRCC, we examined human ccRCC tumor biopsy tissue samples. In ccRCC tissue, high levels of pERK1/2 (Thr202/Tyr204), ERK1/2, pCREB (Ser133), and CREB were observed (Fig. 6a and Supplementary Fig. 6a, b), as well as high intracellular cAMP levels (Fig. 6b). Since ERK1/2 can be

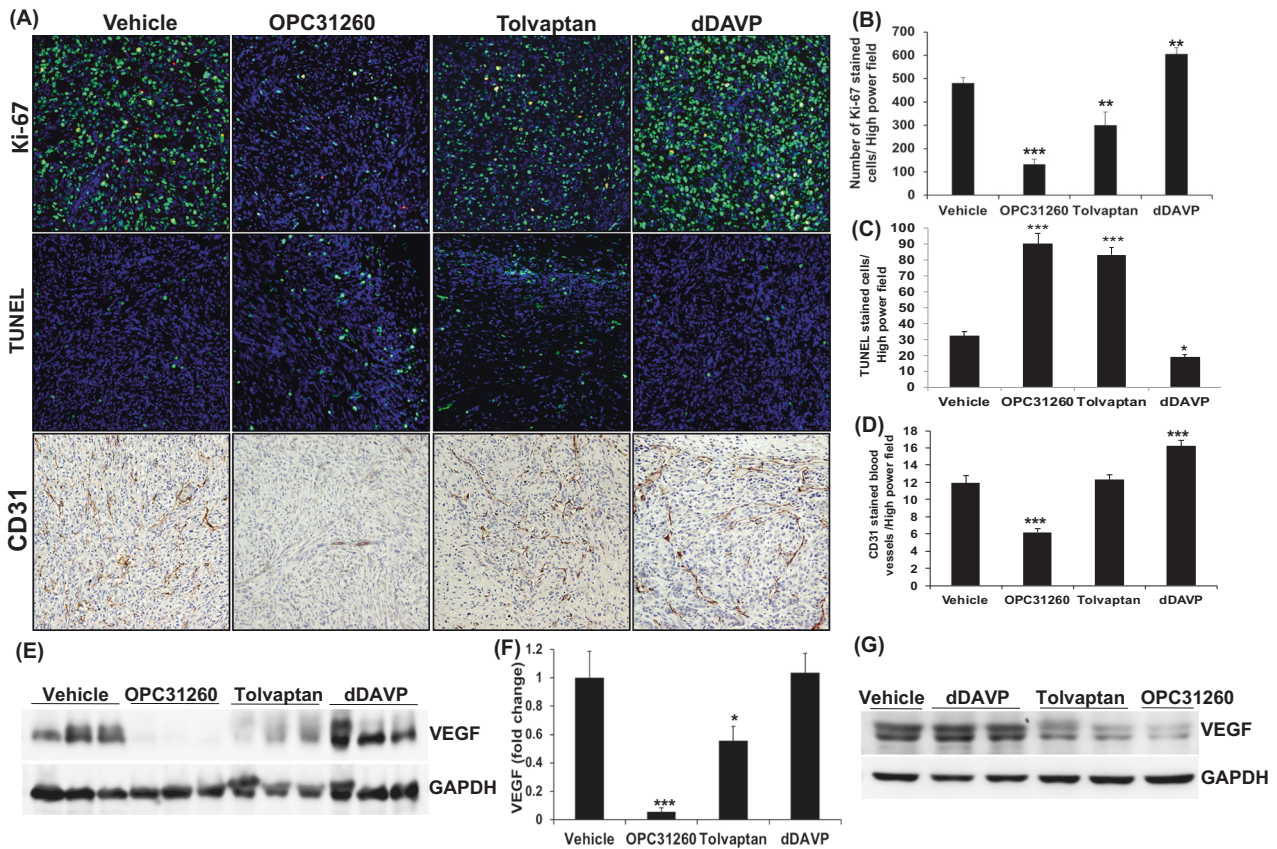


Fig. 5 Effect of V2R agonist or antagonists on RCC tumor cell survival and growth: **a** Ki-67, TUNEL, and CD31 staining in tumors of mice treated with vehicle, OPC31260, Tolvaptan, or dDAVP in tissue sections of tumors from studies in Figs. 3 and 4. **b** Quantification of Ki-67, **c** TUNEL stained cells, and **d** CD31 stained vessels ($n = 4$ tumors each). **e** Western blot for VEGF and **f** Quantification for VEGF

bands by densitometry relative to GAPDH. **g** Western blot for VEGF in Caki-1 cells treated with dDAVP (1 nM), Tolvaptan (50 μ M), and OPC31260 (25 μ M) * $P < 0.05$, ** $P < 0.01$, *** $P < 0.001$ vs Vehicle. All error bars represent SEM. P values by two-tailed unpaired Student's t test with Welch's correction and F test in **b**, **c**, **d**, **f**

regulated by multiple mechanisms in cancer cells, including by V1R [7], we determined the effect of V2R antagonists on ERK1/2 activity. In mouse xenograft tumor tissue lysates, a significant reduction in pERK1/2 was observed in the OPC31260 and Tolvaptan groups, compared with the vehicle treatment groups (Fig. 6c, d, e, f). We next measured intracellular cAMP generation in vitro, since (unlike V1R) activation of V2R induces Gs-mediated adenylate cyclase stimulation resulting in increased intracellular cAMP levels and CREB activity. Short-term treatment with dDAVP significantly increased intracellular cAMP levels in Caki-1 cells, while the V2R antagonists OPC31260 and Tolvaptan significantly reduced cAMP levels (Fig. 6g). Consistently, dDAVP increased pERK1/2 and pCREB levels in Caki-1 cells within 5–30 min after treatment (Fig. 6h), while OPC31260 and Tolvaptan reduced the pERK1/2 and pCREB levels (Fig. 6i). In this study, the V1R antagonist SR49059 showed no effect on pERK1/2 and pCREB levels (Fig. 6i). Cyclic AMP can either be pro- or antiproliferative, depending on the type of cancer. To

further confirm that an increase in intracellular cAMP induces proliferation in ccRCC cells, we determined the effect of cAMP on cell proliferation using the MTT assay. Caki-1 cells were treated with forskolin, a direct activator of adenylate cyclase, which increases intracellular cAMP, or 8-Br-cAMP, a cell permeable cAMP analog. Both treatments significantly increased cell proliferation at 48 h compared with vehicle treated cells (Supplementary Fig. 7).

To further confirm a role for V2R in ccRCC cell growth, we tested the effect of V2R gene silencing in Caki-1 cells. When compared scrambled-SiRNA group, V2R-SiRNA or did not show cell cycle arrest (Fig. 6j, k), but showed significantly reduced cell viability

(Figure 6l) and wound closure (Fig. 6m). Importantly, OPC31260 treatment caused G2/M cell cycle arrest, reduced cell viability, and wound closure in the scrambled-SiRNA group, it failed to do so in the V2R-SiRNA group (Fig. 6k, l, m) consistent with the effect of OPC31260 being through inhibition of V2R.

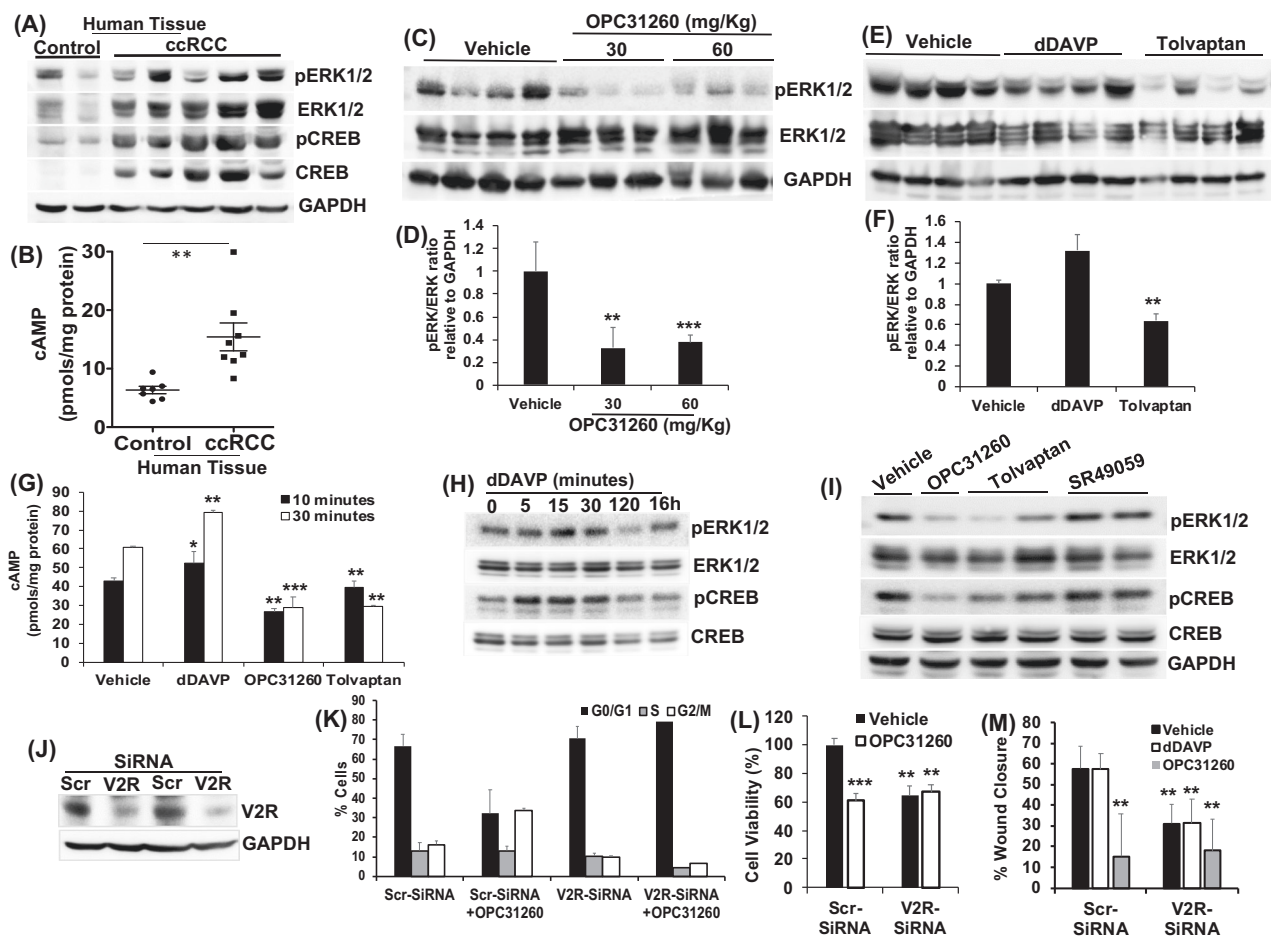


Fig. 6 Effect of V2R agonist and antagonists on angiogenesis in RCC tumors: **a** western blot using control kidney or ccRCC tumor tissue lysate **b** intracellular cAMP of ccRCC tumors and control kidney tissue measured by ELISA ($n = 7$ or 8). **c** Western blot and **d** quantification of band density in tumors of vehicle and OPC31260 treatment groups. **e** Western blot and **f** quantification of band density in tumors of dDAVP and Tolvaptan treatment groups. **g** cAMP levels in Caki-1 cells treated with dDAVP (1 nM), OPC31260 (25 μ M), and Tolvaptan (50 μ M). ($n = 4$ each). **h** Western blot of Caki-1 cells treated with dDAVP (1 nM) or **i** OPC31260 (25 μ M), Tolvaptan (50 μ M), and

SR49059 (10 nM). **j** Western blot for V2R in Caki-1 cells transfected with Scrambled-siRNA (Scr-SiRNA) or V2R-SiRNA. **k** In Caki-1 cells transfected with (Scr-SiRNA) or V2R-SiRNA and treated with vehicle or OPC31260 (25 μ M), cell cycle analysis by FACS, and **l** quantitation of % cells in different cell cycle stages. ($n = 3$) **m** Cell viability by the MTT assay ($n = 12$) and **n** percent wound closure by the scratch assay ($n = 12$). dDAVP (1 nM) was used. * $P < 0.05$, ** $P < 0.01$, *** $P < 0.001$ vs control or vehicle in **b**, **d**, **f**, **g**; vs vehicle treated Scr-SiRNA in **l**, **m**. All error bars represent SD. P values by two-tailed unpaired Student's t test with Welch's correction and F test in **b**, **d**, **f**

Discussion

The present study demonstrates a novel role of the vasopressin type-2 receptor (V2R) in ccRCC tumor growth. Herein, we show for the first time that V2R is abnormally expressed in human ccRCC tumors and plays a pathologic role in driving tumor growth. V2R antagonists were found to reduce cell viability, clonogenicity, and wound closure, and to induce cell cycle arrest of ccRCC cell lines in vitro. Moreover, V2R antagonists suppressed ccRCC tumor growth in a mouse RCC xenograft model by reducing tumor cell proliferation and increasing apoptosis, while a V2R selective agonist had the reverse effect. V2R inhibition was found to reduce cAMP levels, and ERK and CREB activity

in ccRCC cell lines or mouse xenograft tumors. These studies reveal a previously undescribed role of V2R in the pathogenesis of ccRCC, and suggest the possibility of using V2R antagonists, including the FDA-approved drug Tolvaptan as a novel treatment strategy for ccRCC.

While V2R mRNA levels in the TCGA database did not correlate with ccRCC patient survival, our studies demonstrated that V2R is upregulated and can be implicated in the pathology of ccRCC. A recent report citing TCGA data demonstrated a total of nine significantly mutated genes in ccRCC. Mutations in the tumor suppressor PTEN correlates with poor survival in the majority of cancer patients. However, mutant PTEN in ccRCC samples in the TCGA database do not correlate with poor survival. Thus, although

by far, mRNA levels are indicative of the role of a protein in overall survival of cancer patients, there are instances when they do not correlate despite a role in disease pathogenesis [20]. Our observation of abnormal V2R expression in human ccRCC tumors is novel, and consistent with a previous *in vitro* study which showed V2R expression in cultured ccRCC tumor cell lines [11]. We demonstrated V2R mRNA and protein expression in human primary ccRCC tumors and detected V2R expression in tumor cell membranes. It is to be noted that V2R is normally expressed in the collecting duct, distal tubule, and thick ascending limb segments, but not in the proximal tubules of the renal nephrons [16]. Hence V2R expression in ccRCC tumor cells, which are believed to be of proximal tubular origin [12–15], is ectopic, rather than simply being higher in expression when compared with nonmalignant control tissue.

We also detected AVP mRNA expression in human ccRCC tumors. Normally, AVP is synthesized and secreted by specialized neurosecretory cells of the hypothalamus, which have not been described before in normal kidneys, or in ccRCC tumors. Thus, ectopic expression of V2R as well as its ligand could provide a survival and growth advantage to ccRCC tumor cells. Neuropeptide hormones and their receptors are known to be involved in the oncogenic transformation process in various cancers [17]. Ectopic expression of AVP and its receptors has been reported in prostate, colon, breast, small-cell lung carcinoma, gastrointestinal, and head and neck cancers [21, 22]. An abnormal splice variant of V2R, which could negatively regulate normal V2 receptors has also been reported [22, 23]. Based on prior studies, the effect of AVP on tumor growth appears to be dependent on the following: (A) type of cancer: AVP promotes growth of SCLC and breast cancer cell lines *in vitro* [7, 24–26]. *In vivo*, transgenic AVP overexpression increased mammary tumor growth [27], while antibody-mediated targeting of pro-vasopressin impaired SCLC and breast cancer tumor growth in mice [28, 29]. However, in other studies AVP had no growth stimulatory effects on SCLC or adrenocortical tumor cell lines [30–32]. (B) AVP dose: AVP doses of 0.01–1 nM were growth stimulatory, while doses above 10 nM were growth inhibitory in MCF7 breast cancer cell lines [26]. (C) AVP receptor subtype and their postreceptor signaling: the growth-promoting role of AVP on cancer cells is thought to be regulated by V1R via G proteins of the Gq family, and attributed mainly to rise in $[Ca^{++}]_i$ and pERK1/2 levels. Moreover, V1R antagonist treatment reduced AVP-induced proliferation of breast cancer cells [4], while V1R expression in CHO cells which normally do not express AVP receptors increased their cell proliferation [6, 33]. Unlike V1R, V2R activation is generally thought to inhibit cancer cell proliferation because V2R activation increases intracellular cAMP levels, a

known inhibitor of cell proliferation in some cancers [34–38]. However, cAMP is also proproliferative in many types of cancers, and in PKD through stimulation of the ERK pathway [39–45].

Our *in vivo* studies showed that dDAVP can stimulate increases in tumor cell proliferation and tumor growth, and a reduction in tumor cell apoptosis. This observation is consistent with an earlier *in vitro* study in which dDAVP increased proliferation of ccRCC cell lines, which could be blocked by a V2R antagonist [11]. However, dDAVP and its modified analogs reduce tumor metastasis, angiogenesis, and cell proliferation in lung, prostate, breast, and colorectal cancers [8–10, 46–49]. Since dDAVP has greater selectivity for V2R compared with V1R [50], these studies concluded that the effect of dDAVP could be via V2R, and protective in these cancers. Our *in vitro* and *in vivo* studies in ccRCC now show that V2R is growth promoting in ccRCC. While it is currently unclear as to why dDAVP's role in tumor progression is different in breast cancer or small-cell lung carcinoma versus ccRCC, the postreceptor cell-signaling mechanisms could partly explain the difference.

Our studies show that intracellular cAMP and pERK1/2 levels are high in human ccRCC tumors, and can be increased by dDAVP and suppressed by V2R antagonists *in vitro* and *in vivo*. Since V1R activation does not increase cAMP, and because dDAVP, OPC31260, and Tolvaptan are selective for V2R, cAMP mediated activation of ERK1/2 is likely to be the key V2R postreceptor mechanism in ccRCC. The RAS-RAF-MEK-ERK signaling cascade can be activated by multiple mechanisms in cancer cells [51, 52] and its inhibition can reduce tumor growth and angiogenesis in rodent models of RCC [53, 54]. Moreover, sorafenib, a multikinase inhibitor which inhibits RAF-1 and B-RAF, is an approved drug for RCC [55]. We found V1R to be expressed in all human control kidneys and ccRCC tumors. However, SR49059, a V1R inhibitor, failed to reduce pERK1/2 levels in Caki-1 cells, unlike V2R antagonists which did so. Importantly, V2R gene silencing in Caki-1 cells not only reduced cell viability and wound closure, but also abolished the ability of OPC31260 to induce cell cycle arrest or further reduce cell viability and wound closure. These findings suggest that V2R activation can regulate ccRCC tumor growth.

V2R activation in response to AVP is a frequent and normal occurrence in some renal tubular segments, but it does not stimulate cell proliferation or angiogenesis. In fact, dDAVP suppresses cell proliferation related gene expression in normal mouse kidneys [56], because cAMP via PKA inhibits RAF-1, and hence the RAS-RAF-MEK-ERK-signaling pathway, which inhibits cell proliferation [57]. The proproliferative and tumor growth-promoting effects of V2R stimulation in ccRCC in our study is novel, and similar to that in PKD, a disease characterized by abnormal

proliferation of renal tubular epithelial cells causing progressive growth of renal cysts. Unlike ccRCC tumors, cysts in PKD originate mainly from collecting ducts [58] which normally express V2R. In PKD, V2R expression, cAMP, and pERK1/2 mediated cell signaling are enhanced in a setting of low intracellular calcium levels, which allows PKA activation of B-RAF, stimulating increased cell proliferation [57]. Similarities exist in pathogenic mechanisms in PKD and cancers in general [59], and our study adds another by demonstrating that a V2R, cAMP, and ERK1/2 dependent mechanism could be common to PKD and ccRCC.

OPC31260 is about 100 times more selective for V2R than for V1aR [60], while Tolvaptan has 29-fold greater selectivity for human V2R than V1aR [61]. Moreover, Tolvaptan, a structural derivative of OPC31260 does not inhibit V1bR and has no intrinsic V2R agonistic effect [61]. In the current study OPC31260 (30 mg/Kg) had a relatively better effect on reducing tumor size, tumor cell proliferation, and microvessel density and increasing apoptosis compared with Tolvaptan *in vivo*. OPC31260 was also more effective in causing cell cycle arrest, reducing cell viability, and wound closure than Tolvaptan. Although Tolvaptan has relatively better oral activity than OPC31260 [61], it has a mean absolute bioavailability of 56% in humans [62]. This could be the reason for the relatively lower effect of Tolvaptan (oral) compared with OPC31260 (intraperitoneal) in our *in vivo* study. OPC31260 and Tolvaptan doses (30 mg/Kg and 120 mg/Kg respectively) which significantly suppressed ccRCC tumor growth in our study are known to block AVP-dependent V2R activity and reduce urine osmolality in rodents [60, 63]. A dose of 60 mg/Kg of OPC31260 did not show a significantly higher reduction of tumor size, compared with the 30 mg/Kg dose possibly due to target saturation at the lower dose. While the Tolvaptan dose of 120 mg/Kg was higher than the doses of 60 mg/Kg used in normal humans or to treat PKD [62, 64], it should be considered that Tolvaptan treatment is designed to slow kidney enlargement over years or decades of treatment time for PKD, a strategy that is quite different than relatively short-term treatments to stop tumor growth. Tolvaptan treatment could cause side effects including polyuria, thirst or in rare cases, liver toxicity in patients [62, 64]. Although OPC31260 was found to have an IC₅₀ value of 1.2 μM for V2R *in vitro* in isolated rat kidney plasma membranes [60], in our studies, a dose range of 5–10 μM was required to significantly inhibit migration, colony formation and cell viability, and induce cell cycle arrest of Caki-1 and 786-O cells *in vitro*. This could be because higher doses are required in RCC cells to achieve antitumor efficacy. This observation is typical of other repurposed drugs for oncological applications [65, 66].

In our *in vitro* studies, both OPC31260 and Tolvaptan reduced cell viability and wound closure in unstimulated ccRCC cells and reduced tumor growth *in vivo*. In addition, OPC31260 and Tolvaptan also significantly increased tumor cell death by apoptosis, while dDVAP treatment reduced apoptosis compared with vehicle treatment in mouse xenograft tumors. Although the mechanism by which V2R activity regulates tumor cell survival is currently unclear, apoptotic cell death in the V2R antagonist treatment groups could also have contributed to the smaller tumor size. Tolvaptan was recently approved by the US FDA, based on a recent clinical trial for PKD therapy [67]. Thus, while ectopic expression of V2R by ccRCC tumor cells could be an adaptation that gives them a survival and pathogenic advantage, it also makes V2R a potentially useful target of inhibition for ccRCC therapy.

V2R is a homeostatic hormone receptor required for sodium and water balance in the body. Although our study is the first to show a pathologic role for V2R in ccRCC tumor growth, hyponatremia, caused by increased V2R activity, and the syndrome of inappropriate secretion of antidiuretic hormone due to ectopic release of vasopressin are known to occur in hepatocellular, gastric, head and neck, breast, and small-cell lung cancer patients [68, 69]. Moreover, hyponatremia is associated with poorer RCC outcomes and has been proposed to be used as a prognostic indicator or predictive factor [70, 71]. Importantly, Tolvaptan is routinely used for the treatment of hyponatremia in these patients [72]. This is consistent with our data, which suggest that the increased AVP in these cancer patients may be the cause for hyponatremia, and could also be promoting tumor growth.

In summary, our studies demonstrate ectopic expression of V2R and AVP in ccRCC. The V2R agonist dDAVP increased cell proliferation, angiogenesis, and tumor growth, whereas, V2R antagonists OPC31260 and Tolvaptan suppress tumor growth by reducing tumor cell proliferation, increasing apoptosis, and reducing angiogenesis. Although OPC31260 was found to be more effective compared with Tolvaptan, the later is an FDA-approved drug for the treatment of hyponatremia and PKD, and could be repurposed for use in ccRCC therapy.

Materials and methods

Drugs and reagents

Tolvaptan (OPC41061, 7-chloro-5-hydroxy-1-[2-methyl-4-(2-methylbenzoylamino) benzoyl]-2,3,4,5-tetrahydro-1*H*-1-benzazepine), OPC31260 (Mozavaptan, 5-(Dimethylamino)-1-[4-(2-methylbenzamido)benzoyl]-2,3,4,5-tetrahydro-1*H*-benzazepine hydrochloride), 8-Br-cAMP, and

dDAVP (1-desamino-8-d-arginine vasopressin) were from Sigma Millipore (St. Louis, MO). Primary antibodies were purchased for phosphorylated cAMP response element-binding protein (pCREB) (#9198S), CREB (#9197S), Ki-67 (#9449S), phosphorylated extracellular signal regulated kinase (pERK1/2) (#9101S), and ERK1/2 (#SC-94) from Cell Signaling Technology (Danvers, CA, USA); vascular endothelial growth factor (VEGF) (#SC-7269) and GAPDH (#SC-47724) from Santa Cruz Biotechnology (Santa Cruz, CA, USA) and V2R (#V5514) from Sigma Millipore (St. Louis, MO, USA) and CD31 (#ab28364) from Abcam (Cambridge, MA, USA). Secondary antibodies were from Dako (Carpinteria, CA) and ECL reagent was from Perkin Elmer (Waltham, MA, USA).

The cancer genome atlas (TCGA) data analysis

TCGA data were accessed and downloaded through the Xena Genome Browser (University of California Santa Cruz). Subsequent analyzes were conducted in R (v3.5.1) [73] using the *car* and *Rmisc* packages. Figures were constructed using the *ggplot2* package.

Human tumor biopsy tissue

De-identified tissues from surgically removed human ccRCC tumor samples from eight patients, each of whom had pathologically proven ccRCC, and eight nonmalignant control kidney tissues were obtained from the University of Kansas Cancer Center's Biospecimen Core Facility. Our protocols were approved by the Institutional Review Board.

Tumor microarray

TMA array (#KD2082, from US Biomax Inc. Derwood, MD) with 164 ccRCC tumor tissue cores, eight papillary RCC, ten other RCC subtypes (six transitional, three chromophobe and two squamous cell RCCs), ten samples each of cancer-adjacent nonmalignant control and nonmalignant control kidney tissue cores (one specimen per patient). The TMA slide was immunostained for V2R as described below, and V2R staining intensity and immunoreactive areas were scored as 0 (None), 1 (Low), 2 (moderate), or 3 (high). Scoring of tissue cores was performed by a pathologist, blinded to the identity of samples.

Immunostaining

Tumor tissues were fixed and immunofluorescence and immunohistochemistry staining and imaging were performed as described before [58].

cDNA array

A human cDNA array (#HKRT102) consisting of cDNA from 9 control nontumor kidney tissue, 27 ccRCC, and 12 papillary RCC was purchased from OriGene, Rockville, MD. RT-PCR was carried out as following the manufacturer's instructions, and samples were run on 2% agarose gels.

Real-time PCR

RNA was isolated using a Qiagen RNA isolation kit, cDNA was synthesized using a reverse transcription kit from Applied Biosystems, and PCR was performed on an ABI PRISM 7000 sequence detection system (Applied Biosystems, CA). Primers are described in Supplementary Table 1.

Cells

Human ccRCC cell lines 786-O (ATCC-CLR-1932), Caki-1 (ATCC-HTB46), ACHN (ATCC-CLR-1611), and human renal proximal tubular HK-2 (ATCC-CLR-2190) cells were from American Type Culture Collection. 786-O cells were authenticated by STR profiling, and Caki-1 cells were tested for mycoplasma contamination.

Cell viability

Exponentially growing cells in 24-well plates were serum deprived for 16 h, following which the cells were incubated with 0.2% FBS-containing media with vehicle or V2R agonist or antagonists for 48 h. The cells were then incubated in MTT solution (5 mg/mL) for 2 h, following which the MTT solution was washed off and purple formazan solubilized in DMSO and quantified by spectrophotometry at 570 nM. The study was replicated three times, each with $n = 6$ samples.

Clonogenic assay

Cells were plated (1000 cells/well) in six-well plates. After 16 h, cells were treated with different doses of OPC31260. Following 48 h incubation, cells were washed and grown for 10 days until visible colonies formed. Colonies were fixed with a 1:1 ratio of acetone:methanol, stained with 0.25% crystal violet in 25% methanol, washed, air-dried, and photographed. Crystal violet was dissolved in sodium citrate buffer (0.1 M, 50% ethanol, and pH 4.2) and absorbance was measured at 590 nM. The study was replicated three times, each with $n = 2$ samples.

Cell cycle analysis

Cells grown on 100 mm petri dishes were serum deprived for 16 h to synchronize cells, followed by incubation in 1% FBS-containing media in the presence of vehicle or V2R antagonists for 24 h. Cells were then trypsinized, washed twice with PBS, fixed using prechilled 70% ethanol overnight, and permeabilized with PBS containing 0.1% Triton X-100, 1 mg/ml propidium iodide (Sigma-Aldrich, MO), and 2 mg/ml DNase-free RNase at room temperature. Flow cytometry was performed using FACS Calibur analyzer (Becton Dickinson, Mountain View, CA), capturing 10,000 events for each sample. ModFit LT TM software (Verity Software House, Topsham, ME) was used to analyze results. The study was replicated three times, each with $n = 2$ samples.

Wound closure assay

Cells were grown to confluence in six-well plastic plates, then changed to 0.2% FBS-containing medium for 16 h. A scratch-induced wound was then created using a sterile pipet tip. Plates were washed to remove dislodged cells and the same areas of the wounds were photographed at 0 h, and after 24 h of incubation in 0.2% FBS-containing medium. A separate set of plates with similar treatment was used to assess cell proliferation. The study was replicated three times, each with $n = 3$ samples.

Gene silencing using siRNA

V2R-SiRNA (AVPR2-SiRNA) (4390824; Clone 1: S1842, Clone 2: S1843) and Scrambled SiRNA (AM4620) were purchased from Ambion. When the cells were 30–50% confluent, transfections were performed using Lipofectamine[®] RNAiMAX (Invitrogen Carlsbad, CA) following the manufacturer's instructions. For cell cycle analysis, cell viability, and wound closure, experiments were started at 32 h after transfection and continued as described.

Detection of apoptosis/necrosis using Annexin V-FITC/PI staining

Annexin V-FITC/PI staining was performed using the FITC Annexin V apoptosis detection kit (BD Biosciences, USA). Similar studies to cell viability were performed. Cells incubated with OPC31260 for 24 h were washed in cold PBS, resuspended in calcium containing binding buffer (10 mM HEPES, 140 mM NaCl, 5 mM CaCl₂; pH 7.4) at 1×10^6 cells/ml and stained for 15 min, with 5 μ l Annexin V-FITC and 5 μ l PI at 1 μ g/ml. A total of 10,000 cells were analyzed for FITC (excitation 488 nm and emission 530 nm) and PI (610 nm) fluorescence. CellQuestPro[®] software (Becton, Dickinson, Heidelberg, Germany) was

used to determine the percent viable (Annexin V⁻PI⁻), early apoptotic (Annexin V⁺PI⁻), late apoptotic/necrotic (Annexin V⁺PI⁺), and necrotic cells (Annexin V⁻PI⁺). The study was replicated two times, each with $n = 4$ samples.

In vivo xenograft study

All animal studies were carried out according to the protocols approved by the University of Kansas Institutional Animal Care and Use Committee. Female Athymic Nude-Foxn1^{nu} mice, ~25 g and 7–8 weeks old from Envigo/Harlan were subcutaneously injected on the right flank region with 1×10^6 Caki-1 cells in 100 μ l of DMEM medium. Tumor volumes were measured with calipers following the formula, Tumor volume = (length \times width²)/2. When tumor volumes reached ~80–100 mm³, mice were randomized based on their tumor volumes using a randomization chart.

The mice received OPC31260 (30 mg/kg BWt), OPC31260 (60 mg/kg BWt), and dDAVP (1 μ g/kg BWt) by daily intraperitoneal injection [74–76]; or Tolvaptan (120 mg/kg BWt in 1% aqueous solution of hydroxypropyl methylcellulose) by daily oral gavage for 28 days. Vehicle group received saline (50 μ l/20 g mouse, IP) and 1% aqueous solution of hydroxypropyl methylcellulose (200 μ l/20 g mouse, oral gavage). Body weights and tumor volumes were measured every other day. Investigators were not blinded to the identity of the treatments. At the end of the study, tumors were harvested, photographed, weighed, and flash frozen or paraffin embedded for further analysis. Eight mice were used in each group.

Immunoblotting

Tumors tissues or cultured cells were homogenized in SDS Laemmli buffer and immunoblotting was carried out as described before [77].

Measurement of cAMP

Tumors were ground to a fine powder under liquid nitrogen and homogenized in ten volumes of ice cold 0.1 M HCl, and centrifuged at 600 g. In cell culture studies, Caki-1 cells grown on six-well plastic plates were pretreated with IBMX (50 μ M) for 20 min, followed by V1aR and V2R antagonists, or dDAVP (1 nM [11, 78]) treatment for 10 or 30 min. The cells were then washed with ice cold PBS and lysed in 0.1 M HCl. The cAMP levels in tissue and cell extracts were measured as described before [58, 74, 75] using an ELISA kit (#CA-200, Sigma-Aldrich, MO, USA). For tumor tissues, seven control and eight ccRCC tumor tissue were used. The cell culture study was replicated three times, each with $n = 3$ samples.

TUNEL assay for apoptosis

TUNEL assays were performed on tumor sections using an in situ Cell Death Detection Kit (Roche Applied Science, IN, USA) following the manufacturer's instructions. $n = 8$ from each study group.

Statistical analysis

All Statistical analysis was performed using GraphPad Prism, Version 5.0d. Two-way repeated measures of analysis of variance (ANOVA) followed by the Bonferroni test, one-way ANOVA followed by Dunnett's multiple comparison test, or two-tailed unpaired Student's t test with Welch's correction and F test were performed. $P < 0.05$ was considered significant. Data were expressed as mean \pm SEM for in vivo and mean \pm SD for in vitro studies. Sample size estimate was not performed for in vitro studies. Sample size estimate for in vivo studies were made using statistical analysis of power using an online calculator at <https://www.stat.ubc.ca/~rollin/stats/ssize/n2.html>. Sample size of eight mice was determined based on power analysis, to have 95% power, to detect a 50% reduction in tumor weight between vehicle treated and OPC31260 treated mice ($\alpha = 0.05$). Number of samples and study replicates are provided under each method section.

Acknowledgements We thank the University of Kansas Cancer Center Biospecimen Core (P30 CA168524) and the PKD Biomarkers and Biomaterials Core (P30-DK106912) for human specimens, and the Flow Cytometry Core (P30 GM103326 NIH/NIGMS COBRE grant) of University of Kansas Medical Center.

Funding This study was supported by NIH R01-DK083525, a private donation from the Watts family and a Pilot and Feasibility Grant from the KU Cancer Center and PKD Research and Translation Core Center P30-DK106912 to RR. ND is supported by Postdoctoral Fellowship Grants from the KU Biomedical Research and Training Program and American Heart Association.

Compliance with ethical standards

Conflict of interest The authors declare that they have no conflict of interest.

Publisher's note Springer Nature remains neutral with regard to jurisdictional claims in published maps and institutional affiliations.

References

1. Siegel RL, Miller KD, Jemal A. Cancer statistics, 2018. *CA Cancer J Clin.* 2018;68:7–30.
2. Hsieh JJ, Purdue MP, Signoretti S, Swanton C, Albiges L, Schmidinger M, et al. Renal cell carcinoma. *Nat Rev Dis Prim.* 2017;3:17009.
3. Boone M, Deen PM. Physiology and pathophysiology of the vasopressin-regulated renal water reabsorption. *Pflug Arch.* 2008;456:1005–24.

4. Keegan BP, Akerman BL, Pequeux C, North WG. Provasopressin expression by breast cancer cells: implications for growth and novel treatment strategies. *Breast Cancer Res Treat.* 2006;95:265–77.
5. North WG. Gene regulation of vasopressin and vasopressin receptors in cancer. *Exp Physiol.* 2000;85:27S–40S.
6. MacKinnon AC, Tufail-Hanif U, Lucas CD, Jodrell D, Haslett C, Sethi T. Expression of V1A and GRP receptors leads to cellular transformation and increased sensitivity to substance-P analogue-induced growth inhibition. *Br J Cancer.* 2005;92:522–31.
7. Pequeux C, Keegan BP, Hagelstein MT, Geenen V, Legros JJ, North WG. Oxytocin- and vasopressin-induced growth of human small-cell lung cancer is mediated by the mitogen-activated protein kinase pathway. *Endocr Relat Cancer.* 2004;11:871–85.
8. Garona J, Pifano M, Orlando UD, Pastrian MB, Iannucci NB, Ortega HH, et al. The novel desmopressin analogue [V4Q5] dDAVP inhibits angiogenesis, tumour growth and metastases in vasopressin type 2 receptor-expressing breast cancer models. *Int J Oncol.* 2015;46:2335–45.
9. Pifano M, Garona J, Capobianco CS, Gonzalez N, Alonso DF, Ripoll GV. Peptide agonists of vasopressin V2 receptor reduce expression of neuroendocrine markers and tumor growth in human lung and prostate tumor cells. *Front Oncol.* 2017;7:11.
10. Ripoll GV, Garona J, Pifano M, Farina HG, Gomez DE, Alonso DF. Reduction of tumor angiogenesis induced by desmopressin in a breast cancer model. *Breast Cancer Res Treat.* 2013;142:9–18.
11. Bolignano D, Medici MA, Coppolino G, Sciortino MT, Merlo FM, Campo S, et al. Aquaretic inhibits renal cancer proliferation: role of vasopressin receptor-2 (V2-R). *Urologic Oncol.* 2010;28:642–7.
12. Chen F, Zhang Y, Senbabaoglu Y, Ciriello G, Yang L, Reznik E, et al. Multilevel genomics-based taxonomy of renal cell carcinoma. *Cell Rep.* 2016;14:2476–89.
13. Davis CF, Ricketts CJ, Wang M, Yang L, Cherniack AD, Shen H, et al. The somatic genomic landscape of chromophobe renal cell carcinoma. *Cancer Cell.* 2014;26:319–30.
14. Prasad SR, Narra VR, Shah R, Humphrey PA, Jagirdar J, Catena JR, et al. Segmental disorders of the nephron: histopathological and imaging perspective. *Br J Radio.* 2007;80:593–602.
15. Wallace AC, Nairn RC. Renal tubular antigens in kidney tumors. *Cancer.* 1972;29:977–81.
16. Sarmiento JM, Ehrenfeld P, Anazco CC, Reyes CE, Troncoso S, Figueroa CD, et al. Differential distribution of the vasopressin V receptor along the rat nephron during renal ontogeny and maturation. *Kidney Int.* 2005;68:487–96.
17. Heasley LE. Autocrine and paracrine signaling through neuro-peptide receptors in human cancer. *Oncogene.* 2001;20:1563–9.
18. Berl T, Quittnat-Pelletier F, Verbalis JG, Schrier RW, Bichet DG, Ouyang J, et al. Oral tolvaptan is safe and effective in chronic hyponatremia. *J Am Soc Nephrol.* 2010;21:705–12.
19. Chebib FT, Perrone RD, Chapman AB, Dahl NK, Harris PC, Mrug M, et al. A practical guide for treatment of rapidly progressive ADPKD with tolvaptan. *J Am Soc Nephrol.* 2018;29:2458–70.
20. Ricketts CJ, De Cubas AA, Fan H, Smith CC, Lang M, Reznik E, et al. The cancer genome atlas comprehensive molecular characterization of renal cell carcinoma. *Cell Rep.* 2018;23:3698.
21. Khan M, Huang T, Lin CY, Wu J, Fan BM, Bian ZX. Exploiting cancer's phenotypic guise against itself: targeting ectopically expressed peptide G-protein coupled receptors for lung cancer therapy. *Oncotarget.* 2017;8:104615–37.
22. North WG, Fay MJ, Longo KA, Du J. Expression of all known vasopressin receptor subtypes by small cell tumors implies a multifaceted role for this neuropeptide. *Cancer Res.* 1998;58:1866–71.

23. Zhu X, Wess J. Truncated V2 vasopressin receptors as negative regulators of wild-type V2 receptor function. *Biochemistry*. 1998;37:15773–84.
24. Bunn PA, Jr., Chan D, Stewart J, Gera L, Tolley R, Jewett P, et al. Effects of neuropeptide analogues on calcium flux and proliferation in lung cancer cell lines. *Cancer Res*. 1994;54:3602–10.
25. Sethi T, Rozengurt E. Multiple neuropeptides stimulate clonal growth of small cell lung cancer: effects of bradykinin, vasopressin, cholecystokinin, galanin, and neurotensin. *Cancer Res*. 1991;51:3621–3.
26. Taylor AH, Ang VT, Jenkins JS, Silverlight JJ, Coombes RC, Luqmani YA. Interaction of vasopressin and oxytocin with human breast carcinoma cells. *Cancer Res*. 1990;50:7882–6.
27. Chooi KF, Carter DA, Biswas S, Lightman SL, Ho MY, Murphy D. Ectopic vasopressin expression in MMTV-Wnt-1 transgenic mice modifies mammary tumor differentiation and pathology. *Cancer Res*. 1994;54:6434–40.
28. North WG, Cole B, Akerman B, Pang RH. Growth impairment of small-cell cancer by targeting pro-vasopressin with MAG-1 antibody. *Front Oncol*. 2014;4:16.
29. North WG, Pang RH, Gao G, Memoli VA, Cole BF. Native MAG-1 antibody almost destroys human breast cancer xenografts. *Breast Cancer Res Treat*. 2011;127:631–7.
30. Bepler G, Carney DN, Gazdar AF, Minna JD. In vitro growth inhibition of human small cell lung cancer by physalamin. *Cancer Res*. 1987;47:2371–5.
31. Bunn PA, Jr., Chan D, Dienhart DG, Tolley R, Tagawa M, Jewett PB. Neuropeptide signal transduction in lung cancer: clinical implications of bradykinin sensitivity and overall heterogeneity. *Cancer Res*. 1992;52:24–31.
32. Schwindt TT, Forti FL, Juliano MA, Juliano L, Armelin HA. Arginine vasopressin inhibition of cyclin D1 gene expression blocks the cell cycle and cell proliferation in the mouse Y1 adrenocortical tumor cell line. *Biochemistry*. 2003;42:2116–21.
33. Thibonnier M, Conarty DM, Plesnicher CL. Mediators of the mitogenic action of human V(1) vascular vasopressin receptors. *Am J Physiol Heart Circ Physiol*. 2000;279:H2529–39.
34. Cho-Chung YS. Suppression of malignancy targeting cyclic AMP signal transducing proteins. *Biochem Soc Trans*. 1992;20:425–30.
35. Dicitore A, Grassi ES, Caraglia M, Borghi MO, Gaudenzi G, Hofland LJ, et al. The cAMP analogs have potent anti-proliferative effects on medullary thyroid cancer cell lines. *Endocrine*. 2016;51:101–12.
36. Kim SN, Ahn YH, Kim SG, Park SD, Cho-Chung YS, Hong SH. 8-Cl-cAMP induces cell cycle-specific apoptosis in human cancer cells. *Int J Cancer*. 2001;93:33–41.
37. Rocha AS, Paternot S, Coulonval K, Dumont JE, Soares P, Roger PP. Cyclic AMP inhibits the proliferation of thyroid carcinoma cell lines through regulation of CDK4 phosphorylation. *Mol Biol Cell*. 2008;19:4814–25.
38. Shaw TJ, Keszthelyi EJ, Tonary AM, Cada M, Vanderhyden BC. Cyclic AMP in ovarian cancer cells both inhibits proliferation and increases c-KIT expression. *Exp Cell Res*. 2002;273:95–106.
39. Dremier S, Coulonval K, Perpete S, Vandeput F, Fortemaision N, Van Keymeulen A, et al. The role of cyclic AMP and its effect on protein kinase A in the mitogenic action of thyrotropin on the thyroid cell. *Ann N Y Acad Sci*. 2002;968:106–21.
40. Rodrigues AL, Brescia M, Koschinski A, Moreira TH, Cameron RT, Baillie G, et al. Increase in Ca(2+) current by sustained cAMP levels enhances proliferation rate in GH3 cells. *Life Sci*. 2018;192:144–50.
41. Starzec AB, Spanakis E, Nehme A, Salle V, Veber N, Mainguene C, et al. Proliferative responses of epithelial cells to 8-bromo-cyclic AMP and to a phorbol ester change during breast pathogenesis. *J Cell Physiol*. 1994;161:31–8.
42. Takahashi H, Honma M, Miyauchi Y, Nakamura S, Ishida-Yamamoto A, Iizuka H. Cyclic AMP differentially regulates cell proliferation of normal human keratinocytes through ERK activation depending on the expression pattern of B-Raf. *Arch Dermatol Res*. 2004;296:74–82.
43. Tierney T, Robinson IC. Increased lactotrophs despite decreased somatotrophs in the dwarf (dw/dw) rat: a defect in the regulation of lactotroph/somatotroph cell fate? *J Endocrinol*. 2002;175:435–46.
44. Vitali E, Peverelli E, Giardino E, Locatelli M, Lasio GB, Beck-Peccoz P, et al. Cyclic adenosine 3'-5'-monophosphate (cAMP) exerts proliferative and anti-proliferative effects in pituitary cells of different types by activating both cAMP-dependent protein kinase A (PKA) and exchange proteins directly activated by cAMP (Epac). *Mol Cell Endocrinol*. 2014;383:193–202.
45. Zivadinovic D, Gametchu B, Watson CS. Membrane estrogen receptor-alpha levels in MCF-7 breast cancer cells predict cAMP and proliferation responses. *Breast Cancer Res*. 2005;7:R101–12.
46. Alonso DF, Skilton G, Farias EF, Bal de Kier Joffe E, Gomez DE. Antimetastatic effect of desmopressin in a mouse mammary tumor model. *Breast Cancer Res Treat*. 1999;57:271–5.
47. Garona J, Sobol NT, Pifano M, Segatori VI, Gomez DE, Ripoll GV, et al. Preclinical efficacy of [V4Q5]dDAVP, a second generation vasopressin analog, on metastatic spread and tumor-associated angiogenesis in colorectal cancer. *Cancer Res Treat*. 2019;51:438–50.
48. Giron S, Tejera AM, Ripoll GV, Gomez DE, Alonso DF. Desmopressin inhibits lung and lymph node metastasis in a mouse mammary carcinoma model of surgical manipulation. *J Surg Oncol*. 2002;81:38–44.
49. Iannucci NB, Ripoll GV, Garona J, Cascone O, Ciccia GN, Gomez DE, et al. Antiproliferative effect of 1-deamino-8-D-arginine vasopressin analogs on human breast cancer cells. *Future Med Chem*. 2011;3:1987–93.
50. Zaoral M. Vasopressin analogs with high and specific antidiuretic activity. *Int J Pept Protein Res*. 1985;25:561–74.
51. Ryan MB, Der CJ, Wang-Gillam A, Cox AD. Targeting RAS-mutant cancers: is ERK the key? *Trends Cancer*. 2015;1:183–98.
52. Santarpia L, Lippman SM, El-Naggar AK. Targeting the MAPK-RAS-RAF signaling pathway in cancer therapy. *Expert Opin Ther Targets*. 2012;16:103–19.
53. Chang YS, Adnane J, Trail PA, Levy J, Henderson A, Xue D, et al. Sorafenib (BAY 43-9006) inhibits tumor growth and vascularization and induces tumor apoptosis and hypoxia in RCC xenograft models. *Cancer Chemother Pharmacol*. 2007;59:561–74.
54. Huang D, Ding Y, Luo WM, Bender S, Qian CN, Kort E, et al. Inhibition of MAPK kinase signaling pathways suppressed renal cell carcinoma growth and angiogenesis in vivo. *Cancer Res*. 2008;68:81–8.
55. Kane RC, Farrell AT, Saber H, Tang S, Williams G, Jee JM, et al. Sorafenib for the treatment of advanced renal cell carcinoma. *Clin Cancer Res*. 2006;12:7271–8.
56. Cai Q, McReynolds MR, Keck M, Greer KA, Hoying JB, Brooks HL. Vasopressin receptor subtype 2 activation increases cell proliferation in the renal medulla of AQP1 null mice. *Am J Physiol Ren Physiol*. 2007;293:F1858–64.
57. Yamaguchi T, Wallace DP, Magenheimer BS, Hempson SJ, Grantham JJ, Calvet JP. Calcium restriction allows cAMP activation of the B-Raf/ERK pathway, switching cells to a cAMP-dependent growth-stimulated phenotype. *J Biol Chem*. 2004;279:40419–30.
58. Tao S, Kakade VR, Woodgett JR, Pandey P, Suderman ED, Rajagopal M, et al. Glycogen synthase kinase-3beta promotes cyst expansion in polycystic kidney disease. *Kidney Int*. 2015;87:1164–75.
59. Seeger-Nukpezah T, Geynisman DM, Nikonova AS, Benzing T, Golemis EA. The hallmarks of cancer: relevance to the

- pathogenesis of polycystic kidney disease. *Nat Rev Nephrol*. 2015;11:515–34.
60. Yamamura Y, Ogawa H, Yamashita H, Chihara T, Miyamoto H, Nakamura S, et al. Characterization of a novel aquaretic agent, OPC-31260, as an orally effective, nonpeptide vasopressin V2 receptor antagonist. *Br J Pharmacol*. 1992;105:787–91.
 61. Kondo K, Ogawa H, Yamashita H, Miyamoto H, Tanaka M, Nakaya K, et al. 7-Chloro-5-hydroxy-1-[2-methyl-4-(2-methyl-benzoyl-amino)benzoyl]-2,3,4,5-tetrahydro-1H-1-benzazepine (OPC-41061): a potent, orally active nonpeptide arginine vasopressin V2 receptor antagonist. *Bioorg Med Chem*. 1999;7:1743–54.
 62. Shoaf SE, Kim SR, Bricmont P, Mallikaarjun S. Pharmacokinetics and pharmacodynamics of single-dose oral tolvaptan in fasted and non-fasted states in healthy Caucasian and Japanese male subjects. *Eur J Clin Pharmacol*. 2012;68:1595–603.
 63. Aihara M, Fujiki H, Mizuguchi H, Hattori K, Ohmoto K, Ishikawa M, et al. Tolvaptan delays the onset of end-stage renal disease in a polycystic kidney disease model by suppressing increases in kidney volume and renal injury. *J Pharmacol Exp Ther*. 2014;349:258–67.
 64. Watkins PB, Lewis JH, Kaplowitz N, Alpers DH, Blais JD, Smotzer DM, et al. Clinical pattern of tolvaptan-associated liver injury in subjects with autosomal dominant polycystic kidney disease: analysis of clinical trials database. *Drug Saf*. 2015;38:1103–13.
 65. Pantziarka P, Bouche G, Meheus L, Sukhatme V, Sukhatme VP, Vikas P. The repurposing drugs in oncology (ReDO) project. *Ecancermedicallscience*. 2014;8:442.
 66. Seo EJ, Sugimoto Y, Greten HJ, Efferth T. Repurposing of bromocriptine for cancer therapy. *Front Pharmacol*. 2018;9:1030.
 67. Torres VE, Chapman AB, Devuyst O, Gansevoort RT, Perrone RD, Koch G, et al. Tolvaptan in later-stage autosomal dominant polycystic kidney disease. *New Engl J Med*. 2017;377:1930–42.
 68. Burst V, Grundmann F, Kubacki T, Greenberg A, Rudolf D, Salahudeen A, et al. Euvolemic hyponatremia in cancer patients. Report of the Hyponatremia Registry: an observational multicenter international study. *Support Care Cancer*. 2017;25:2275–83.
 69. Onitilo AA, Kio E, Doi SA. Tumor-related hyponatremia. *Clin Med Res*. 2007;5:228–37.
 70. Bellmunt J, Leow JJ. Hyponatremia associated with worse outcomes in metastatic renal cell cancer: a potential target for intervention? *Eur Urol*. 2014;65:731–2.
 71. Jeppesen AN, Jensen HK, Donskov F, Marcussen N, von der Maase H. Hyponatremia as a prognostic and predictive factor in metastatic renal cell carcinoma. *Br J Cancer*. 2010;102:867–72.
 72. Gralla RJ, Ahmad F, Blais JD, Chiodo J 3rd, Zhou W, Glaser LA, et al. Tolvaptan use in cancer patients with hyponatremia due to the syndrome of inappropriate antidiuretic hormone: a post hoc analysis of the SALT-1 and SALT-2 trials. *Cancer Med*. 2017;6:723–9.
 73. R Development Core Team. R: a language and environment for statistical computing. R Foundation for Statistical Computing, Vienna, Austria. R Foundation for Statistical Computing, Vienna; 2014.
 74. Kakade VR, Tao S, Rajagopal M, Zhou X, Li X, Yu AS, et al. A cAMP and CREB-mediated feed-forward mechanism regulates GSK3beta in polycystic kidney disease. *J Mol Cell Biol*. 2016;8:464–76.
 75. Rao R, Patel S, Hao C, Woodgett J, Harris R. GSK3beta mediates renal response to vasopressin by modulating adenylate cyclase activity. *J Am Soc Nephrol*. 2010;21:428–37.
 76. Shi PP, Cao XR, Qu J, Volk KA, Kirby P, Williamson RA, et al. Nephrogenic diabetes insipidus in mice caused by deleting COOH-terminal tail of aquaporin-2. *Am J Physiol Ren Physiol*. 2007;292:F1334–44.
 77. Singh SP, Tao S, Fields TA, Webb S, Harris RC, Rao R. Glycogen synthase kinase-3 inhibition attenuates fibroblast activation and development of fibrosis following renal ischemia-reperfusion in mice. *Dis Models Mech*. 2015;8:931–40.
 78. Gunaratne R, Braucht DW, Rinschen MM, Chou CL, Hoffert JD, Pisitkun T, et al. Quantitative phosphoproteomic analysis reveals cAMP/vasopressin-dependent signaling pathways in native renal thick ascending limb cells. *Proc Natl Acad Sci USA*. 2010;107:15653–8.